Dyes and Pigments 254 (2026) 113981

Contents lists available at ScienceDirect

Dyes and Pigments

journal homepage: www.elsevier.com/locate/dyepig

Photodynamic inactivation mediated by TMPyP and potassium iodide: A promising strategy for *Vibrio anguillarum* control in aquaculture

Cátia Vieira [a], Maria Bartolomeu [a,b], Pedro P. Gallego [c], M. Graça P.M. S. Neves [d], Jesús L. Romalde [e,*], M. Amparo F. Faustino [d,**], Adelaide Almeida [a,***]

[a] CESAM, Department of Biology, University of Aveiro, Campus Universitário de Santiago, Aveiro, 3810-193, Portugal
[b] Centre for Interdisciplinary Research in Health (CIIS), Universidade Católica Portuguesa, Faculty of Dental Medicine, Viseu, 3504-505, Portugal
[c] Agrobiotech for Health, Plant Biology and Soil Science Department, Biology Faculty, University of Vigo, Vigo, Spain
[d] LAQV-REQUIMTE, Department of Chemistry, University of Aveiro, Campus Universitário de Santiago, Aveiro, 3810-193, Portugal
[e] Cross-disciplinary Research Center in Environmental Technologies (CRETUS), Department of Microbiology and Parasitology, CIBUS-Faculty of Biology, University of Santiago de Compostela, Santiago de Compostela, 15782, Spain

ARTICLE INFO

Keywords:
Antimicrobial photodynamic inactivation
Fish
Artemia franciscana
Scophthalmus maximus
Seawater
Decontamination

ABSTRACT

Vibrio anguillarum is a pathogenic bacterium associated with high mortality rates and economic losses in the aquaculture sector. This bacterium is often found in brine shrimp nauplii, a common live food for fish, making it a notable vector for pathogen transmission. This study aimed to evaluate the potential of antimicrobial photodynamic inactivation (aPDI) as a proof-of-concept approach for decontamination and prophylactic control of *V. anguillarum* infections in aquaculture. To accomplish this, the efficiency of aPDI was assessed in: i) photoinactivating *V. anguillarum* in seawater; ii) decontaminating brine shrimp nauplii (*Artemia franciscana)* contaminated with *V. anguillarum;* and iii) preventing infections in turbot (*Scophthalmus maximus* L.) prechallenged with *V. anguillarum*. These experiments employed the tetracationic photosensitizer 5,10,15,20-tetrakis(1-methylpyridinium-4-yl)porphyrin (TMPyP; 5.0 μM), combined with the well-known aPDI adjuvant potassium iodide (KI, 10-100 mM), under white light irradiation (100 mW cm^{-2}). For the *in vivo* assays, treatment conditions were selected through toxicity assays and then applied to brine shrimp nauplii and turbot juveniles artificially contaminated with *V. anguillarum*. The results showed that aPDI mediated by TMPyP + KI efficiently reduced *V. anguillarum* concentration in seawater to undetectable levels in less than 10 min. Toxicity assays confirmed that TMPyP (5.0 μM) + KI (10 mM) did not induce detectable adverse effects in turbot and brine shrimp under the tested conditions. This combination also significantly reduced bacterial loads on brine shrimp nauplii (>3 log CFU mL^{-1}) after 30 min. In turbot trials, a 5-min treatment was associated with an attenuation of disease symptoms but did not result in a statistically significant reduction in mortality. Overall, aPDI showed strong potential for reducing *V. anguillarum* contamination in seawater and live food, supporting its applicability as an environmental decontamination and prophylactic strategy. However, its effectiveness in directly preventing an stablished fish infection appears limited under the tested conditions and may require an earlier or repeated application. Further studies should focus on optimizing timing, dosage, and delivery protocols to improve in *vivo* protection prophylactic efficacy.

1. Introduction

Vibriosis, an infectious disease caused by bacteria of the *Vibrionaceae* family, poses a significant threat to farmed fish populations [1]. In particular, *Vibrio anguillarum* is responsible for causing severe outbreaks in turbot (*Scophthalmus maximus*) aquaculture, leading to high mortality rates and significant economic losses [2,3]. Infected fish commonly develop ulcers on the fins and gills and may succumb to fatal

* Corresponding author.
** Corresponding author.
*** Corresponding author.
E-mail addresses: catiavieira@ua.pt (C. Vieira), maria.bartolomeu@ua.pt (M. Bartolomeu), pgallego@uvigo.es (P.P. Gallego), gneves@ua.pt (M.G.P.M.S. Neves), jesus.romalde@usc.es (J.L. Romalde), faustino@ua.pt (M.A.F. Faustino), aalmeida@ua.pt (A. Almeida).

https://doi.org/10.1016/j.dyepig.2026.113981
Received 6 April 2026; Received in revised form 25 June 2026; Accepted 26 June 2026
Available online 27 June 2026

haemorrhagic septicaemia [4]. *V. anguillarum* infects turbot by penetrating the skin and mucous membranes or through the ingestion of contaminated water or food [4,5]. Brine shrimp nauplii, a common live food, are frequently implicated as a significant vector for *V. anguillarum* transmission to farmed fish [6]. During the initial stages of infection, the bacterium first colonizes the stomach before reaching the intestine, where it proliferates. It then crosses the intestinal epithelium via endocytosis. Once inside, the pathogen can enter the bloodstream, leading to septicaemia or spreading to various organs, such as liver, spleen, and kidney [4,5].

Currently, antibiotics and vaccines are the primary strategies employed to control infections caused by *V. anguillarum* [2,7]. However, due to the variability among *V. anguillarum* strains, existing vaccines may not provide full protection. Furthermore, antibiotic efficacy is declining due to the rise of antimicrobial resistance, and their use is increasingly discouraged because of their negative environmental impact [8–10]. In addition, water and fish food decontamination methods (e.g., ozone, chlorine, and ultraviolet radiation [UV]) serve as additional biosecurity measures to prevent microbial outbreaks [11]. However, these methods can generate toxic byproducts, contribute to the development of resistant strains, and pose risks to aquatic life [12–14]. Consequently, the development of innovative and sustainable antimicrobial approaches is crucial to prevent *V. anguillarum* infections in turbot.

Given the limitations of conventional disease control strategies, antimicrobial Photodynamic Inactivation (aPDI), has gained attention as an effective and sustainable antimicrobial approach [15–19]. The mechanism of aPDI relies on the use of a photosensitizer (PS), a dye that, when excited by visible light in the presence of dioxygen ($^3O_2$), generates reactive oxygen species (ROS) [20–22]. These ROS oxidize bacterial structures, ultimately leading to cell death [18,23,24]. aPDI has been shown to photoinactivate fish pathogenic bacteria making it a compelling candidate for aquaculture applications [25–31]. However, its direct application for treating established infections in farmed fish remains largely unexplored. To the best of our knowledge, only one study has investigated the use of aPDI to treat bacterial infections in fish [32]. That study demonstrated that an aggregation-induced emission PS, TTCPy-3, was effective in treating zebrafish (*Danio rerio*) infected with the intracellular Gram-positive bacterium *Nocardia seriolae* [32]. Recently, our research group showed that aPDI mediated by the standard tetracationic porphyrin 5,10,15,20-tetrakis(1-methylpyridinium-4-yl)porphyrin (TMPyP), in combination with potassium iodide (KI), a well-known aPDI coadjuvant, was effective in photoinactivating fish pathogenic bacteria (*Vibrio parahaemolyticus* and *V. anguillarum*) in artificial seawater and fish fillet [25,33]. These findings suggest that aPDI could also be effective when directly applied in aquaculture systems for infection prevention.

This study aimed to assess, for the first time, the potential of aPDI mediated by TMPyP, alone and in combination with KI, in controlling *V. anguillarum* infections in aquaculture under *in vivo* conditions. To this purpose, the efficiency of aPDI treatments was investigated in: (a) photoinactivating *V. anguillarum* in seawater; (b) decontaminating brine shrimp (*Artemia franciscana*) nauplii contaminated with *V. anguillarum*; and (c) preventing infections in turbot (*Scophthalmus maximus*) challenged with *V. anguillarum*.

2. Materials and Methods

2.1. Photosensitizer and KI solution

The porphyrin TMPyP was synthesized according to the literature [34]. Stock solutions of this PS (see structure in Fig. 1) were prepared at 500 μM in dimethyl sulfoxide (DMSO) and maintained in the dark at room temperature. Before each experiment, the stock solution was sonicated for 30 min at room temperature using an ultrasonic bath (Sonorex Super RK 31, 35 kHz, Bandelin, Germany). KI was purchased from Scharlab (Barcelona, Spain), and the solutions were prepared at 5 M in sterile phosphate buffer solution (PBS), immediately before each experiment.

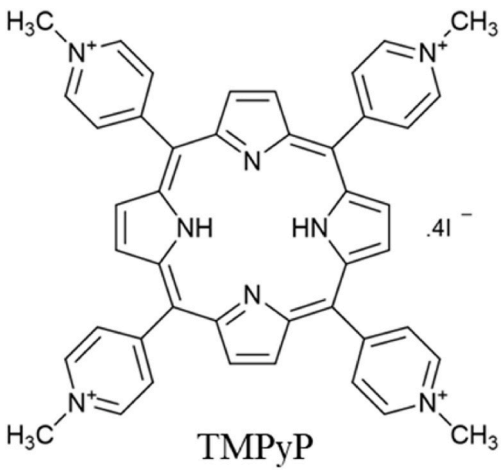

Fig. 1. Structure of TMPyP.

2.2. Bacterial strain, brine shrimp, and turbot culture conditions

Antimicrobial photodynamic inactivation treatments were performed on *V. anguillarum* strain previously isolated from a turbot farm located in O Grove, Spain (latitude 42°28′16″N & longitude 8°51′42″W). The bacterium was maintained on tryptic soy agar (TSA, Liofilchem, Roseto d. Abruzzi, Italy) supplemented with 1 % of NaCl at 4 °C. Before each assay, two isolated colonies were transferred to 20 mL of Tryptic Soy Broth (TSB, Liofilchem, Roseto d. Abruzzi, Italy) supplemented with 1 % of NaCl and were overnight incubated at 25 °C under orbital stirring (120 rpm). Then, 200 μL of the previous suspension were transferred to fresh 20 mL TSB and incubated at the previously mentioned conditions until the stationary phase of approximately 10^9 colony-forming units per mL (CFU mL^{-1}) was reached.

Brine shrimp nauplii were prepared according to Sorgeloos et al. (1977) with some modifications [35]. Brine shrimp cysts (Aquapex - Artemia "PRO") were maintained under refrigeration (4 °C) [35]. Before each assay, the cysts were placed in 6-well plates and hydrated in 10 mL of sterile filtrated seawater (35 g/L) at a density of 0.05 g mL^{-1}. The samples were maintained under continuous white-light irradiation (100 mW cm^{-2}) at 25 °C for 48 h without stirring to promote hatching. Within 24 h after hatching, the brine shrimp nauplii were washed three times with sterile filtrated seawater to remove residual organic matter and reduce natural contamination.

Turbot fingerlings (n = 100; average weight: 10 ± 2.3 g) were purchased from a commercial hatchery and maintained at the aquarium facilities of the Faculty of Biology at University of Santiago of Compostela in 200 L seawater tanks at 18 ± 2 °C, with a salinity ranging from 28 to 30 g L^{-1} and a photoperiod of 12 h light:12 h dark. Fish were acclimated for 15 days prior to treatment, and their health status was monitored by observing external appearance, swimming behaviour, and appetite. The fish were fed commercial pellets (Skretting, Stavanger, Norway) according to the supplier's recommendations. Seawater was collected from the coastal region of Galicia, Spain, and its quality was maintained using mechanical filtration (sand and activated charcoal filters).

2.3. Light source

The experiments were performed under white light irradiation (emission spectrum of 380 – 700 nm), provided by an LED system LUMECO (30 W, 2000 lm, China). A PowerMeter Coherent FieldMaxII-

Top combined with a Coherent PowerSens PS19Q energy sensor was used to measure and adjust the light irradiance to 100 mW cm^{-2} [25,33,36].

2.4. Photodynamic inactivation procedure in seawater

The photodynamic inactivation of *V. anguillarum* was evaluated using TMPyP alone at 5.0 μM and in combination with KI at 10, 50 and 100 mM. The concentrations were selected according to the literature to ensure biological activity without host toxicity [15,25,37,38]. These concentrations were selected based on previous studies [25,39,40].

An overnight culture of *V. anguillarum* (~10^9 CFU mL^{-1}) was diluted 10-fold in seawater to a final concentration of 10^8 CFU mL^{-1} (collected from the aquarium facilities), and transferred to 12-well plates. TMPyP alone and in combination with KI were added to achieve the selected concentrations. In parallel, light and dark controls were included to assess the effects of irradiation and compound toxicity: (i) light controls, consisting of the bacterial suspension alone (LC) or with KI at the highest tested concentration (LC + KI), both subjected to irradiation; and (ii) a dark control (DC), containing the bacterial suspension with TMPyP and KI at the highest tested concentration, protected from light exposure.

Samples were incubated in the dark under stirring for 10 min to facilitate TMPyP binding to *V. anguillarum* cells [15,28,41]. Then, samples and light controls were irradiated for 10 min with white light (380–700 nm, 100 mW cm^{-2}), while the dark control remained shielded from light exposure. At time 0 (immediately after the 10 min of dark incubation) and at various points during irradiation (5, 6, 7, and 10 min), aliquots were collected, serially diluted in PBS, and drop-plated in duplicate (10 μL) on TSA supplemented with 1 % NaCl. Plates were incubated at 25 °C for 48 h, after which viable colony counts were determined and expressed as CFU mL^{-1}. The detection limit of method was 2 log CFU mL^{-1}, corresponding to the absence of colonies on the lowest dilution plated. Three independent experiments were conducted with two replicates, and the results were averaged.

2.5. Brine shrimp experiments

2.5.1. Toxicity screening of aPDI treatments in brine shrimp nauplii

In this study, the toxicity of the aPDI treatments toward brine shrimp nauplii was evaluated as a preliminary screening to select suitable conditions for live food decontamination. For this purpose, brine shrimp nauplii within 24 h of hatching were transferred to 12-well plates containing 4.0 mL of sterile seawater (10 individuals per well). Treatments consisting of TMPyP (5.0 μM) and KI (10, 50, and 100 mM), both alone and in combination, were added to the corresponding wells. A control group containing only brine shrimp nauplii without treatment was also included (LC). The plates were then irradiated with white light (100 mW cm^{-2}) for 60 min. Simultaneously, identical treatments were prepared in 12-well plates and maintained in the dark during the irradiation procedure to serve as dark controls (DC). Toxicity was assessed by observing the motility (active swimming vs. immobility), morphological alterations (body deformations, including alterations in shape and structural integrity) and mortality (absence of appendage movement) of individuals immediately after irradiation and again after 24 h to determine long-term effects. Survival was calculated as the percentage of live nauplii divided by the total number of nauplii. Morphological alterations were analysed using a Nikon ECLIPSE 80i microscope equipped with a 10× objective, a Nikon Digital Sight DS-U3 data acquisition system, and a Nikon Digital Sight DS-Ri1 camera (Tokyo, Japan). Three independent experiments were conducted with three replicates, and the results were averaged.

2.5.2. Accumulation of V. anguillarum in brine shrimp nauplii

The brine shrimp nauplii were artificially contaminated with *V. anguillarum* to simulate contaminated live food and to evaluate the effectiveness of TMPyP- and TMPyP + KI-mediated aPDI treatments. Using a Pasteur pipette, brine shrimp nauplii were transferred to 6-well plates containing 10 mL of sterile seawater with *V. anguillarum* (10^9 CFU mL^{-1}) and incubated for 3 h according to previous studies [42,43]. To assess bacterial accumulation, 10 nauplii were collected, rinsed three times with sterile seawater, and homogenized using a micropestle. Then, these suspensions were serially diluted and plated by both drop-plating (10 μL) and spread-plating (100 μL) on TSA supplemented with 1 % NaCl and thiosulfate citrate bile salts sucrose agar (TCBS, Liofilchem, ISO 21872, Roseto degli Abruzzi, Italy) to assess total viable bacteria and *Vibrio* populations, respectively. The bacterial concentration was expressed as log CFU mL^{-1}. Control samples consisting of nauplii not exposed to *V. anguillarum* were included to determine the natural microbial concentration. Three independent experiments were conducted with three replicates, and the results were averaged.

To confirm bacterial internalization, brine shrimp nauplii were examined by epifluorescence microscopy following exposure to *V. anguillarum* labelled with acridine orange [44,45]. Bacterial suspensions were prepared in sterile seawater (~10^9 CFU mL^{-1}) and incubated in the dark with acridine orange (20 mg L^{-1}) under orbital agitation for 15 min to allow dye binding to bacterial cells. After incubation, the suspension was centrifuged for 5 min at 13,000 rpm (1730R, Gyrozen Co., Ltd., Gimpo, South Korea) [25,46], and the supernatant containing unbound dye was discarded. The bacterial pellet was washed three times with sterile seawater, followed by centrifugation under the same conditions. The fluorescently labelled bacterial cells were then added to 6-well plates containing brine shrimp nauplii in sterile seawater and incubated for 3 h. Following incubation, nauplii were washed three times with sterile water to remove non-adherent bacteria and analysed by epifluorescence microscopy. Imaging was performed using a Nikon ECLIPSE 80i microscope equipped with a 10× objective, a Nikon Digital Sight DS-U3 data acquisition system, and a Nikon Digital Sight DS-Ri1 camera (Tokyo, Japan). A FITC filter set (EX 465–495, DM 505, BA 515–555) was used to detect acridine orange fluorescence.

2.5.3. Photodynamic treatment of V. anguillarum in brine shrimp nauplii

Artificially contaminated brine shrimp nauplii were transferred to 12-well plates (10 nauplii per well, totaling 90 individuals per condition) using a Pasteur pipette. Each well contained sterile seawater with predetermined non-toxic concentrations of: TMPyP at 5.0 μM,and TMPyP at 5.0 μM in combination with KI at 10 mM. These samples were incubated in the dark for 10 min, followed by white light irradiation (100 mW cm^{-2}) for 10, 30, and 60 min. Simultaneously, two light control groups were included: one with brine shrimp nauplii alone (LC) and another with brine shrimp nauplii and KI (LC + KI), both irradiated. A dark control group, consisting of individuals treated with TMPyP at 5.0 μM and KI at 10 mM but protected from light exposure, was also included (DC). After irradiation, the bacterial concentration in nauplii was assessed as previously described in section 2.5.2. and expressed as log CFU mL^{-1}. Three independent experiments were conducted with three replicates, and the results were averaged.

2.6. Turbot fingerlings experiments

2.6.1. Determination of toxicity

The toxicity of treatments was tested by transferring five turbot fingerlings to tanks containing 2.0 L of seawater. TMPyP and/or KI aliquots were added to achieve final concentrations of 5.0 μM and 10–50 mM, respectively. Following a 10-min dark incubation period and 5 min of aPDI irradiation within 2 L tanks, the fish were transferred to acclimatized 200 L tanks (conditions previously described in section 2.2 of Materials and Methods), where their behaviour and mortality were evaluated over 24 h. A control group of untreated fish was also included for comparison.

2.6.2. Photodynamic treatment of turbot challenged with V. anguillarum

The assessment of aPDI effects on turbot challenged with

V. anguillarum followed the protocol illustrated in Fig. 2. Prior to the experiments, individuals (n = 5) were transferred to 2.0 L tanks and immersion-challenged with a lethal dose of *V. anguillarum* (10^7 CFU mL^{-1}) for 30 min [47]. After this period, TMPyP and KI were added to the tanks to achieve final concentrations of 5.0 μM and 10 mM, respectively. Following a dark incubation period of 10 min, the fish were irradiated in the aquaria for 5 min (380–700 nm, 100 mW cm^{-2}) and then transferred to 200 L acclimatized seawater tanks (conditions previously described in section 2.2 of Materials and Methods) (Fish_TMPyP + KI_Light). Considering the limited number of turbot fingerlings available, only the combined treatment of TMPyP and KI was tested in these assays, as previous experiments in seawater demonstrated its effectiveness to be equal to or superior to TMPyP alone. Four control groups were included: (i) fish not challenged with *V. anguillarum* (Non-Infected Fish); (ii) infected fish without any treatment (Fish); (iii) infected fish exposed to the same irradiation protocols as the treated samples (Fish_Light); and (iv) infected fish treated with TMPyP and KI but protected from light exposure (Fish_TMPyP + KI_Dark). In all these assays, three replicates were performed per condition.

To confirm bacterial concentration and assess immediate aPDI effect on free-swimming bacteria in seawater, aliquots of 1.0 mL were collected from each treatment tank before and after irradiation, and the *V. anguillarum* concentration was assessed as previously described in section 2.4.

To evaluate the effect of the treatments, each individual's behaviour (swimming ability and activity), motility, and symptoms were assessed immediately after treatment and over 9 days. This period was defined as the experimental endpoint since no additional mortality was observed after day 7 in either the control or treated groups. Diseased animals were dissected using a sterile scalpel to collect the kidney and liver. The presence of *V. anguillarum* in ulcers (skin, fins, and gills) and kidneys was assessed by streaking samples collected with a sterile loop onto TCBS agar. Positive samples were confirmed via biochemical identification using the API 20E (bioMérieux, Inc.). Three replicates were performed per condition.

2.7. Statistic analysis

GraphPad Prism 8.0.1 was used to perform statistical analysis. Normal distributions and homogeneity of variance were assessed with the Shapiro-Wilk and the Brown–Forsythe test, respectively. Two-way analysis of variance (two-way ANOVA) followed by Tukey's multiple comparison test were applied to evaluate the effects of the different treatments and exposure time (10, 30, and 60 min), as well as their interaction. A value of $p < 0.05$ was considered statistically significant. Three independent assays were performed for each condition.

3. Results

3.1. Photoinactivation of V. anguillarum in seawater

The results of *V. anguillarum* photoinactivation in seawater using TMPyP and TMPyP + KI are summarized in Fig. 3. No significant changes were observed in the light control (LC) or dark control (DC) groups ($p > 0.05$). These results indicate that *V. anguillarum* viability was not affected by irradiation alone, by KI (100 mM) exposed to light, or by the PS (5.0 μM) combined with KI (100 mM) in the dark.

TMPyP at 5.0 μM alone was highly effective, reducing the bacterial concentration by 3.0 and 7.0 log CFU mL^{-1} after 7 and 10 min of white light irradiation, respectively. The addition of KI further enhanced the photodynamic effect of TMPyP, achieving bacterial reduction to the detection limit of the method after 5, 6, and 7 min of treatment at KI concentrations of 100, 50, and 10 mM, respectively.

3.2. Brine shrimp experiments

3.2.1. Toxicity of TMPyP and KI

The toxicity of TMPyP (5.0 μM), alone and in combination with KI (10, 50, and 100 mM), was evaluated in brine shrimp nauplii immediately after treatment and again after 24 h. Individuals were considered dead if no motility in the appendage was observed or if they exhibited severe and irreversible deformities. The results indicate that TMPyP alone did not induce detectable adverse effects in brine shrimp nauplii under the tested conditions (Table 1, Fig. 4). However, nauplii exposed to high concentrations of KI showed adverse effects. Reduced swimming activity and increased lethargy were observed immediately after treatment with KI at 50 and 100 mM. Additionally, delayed growth and morphological alterations in the antennae and thorax became evident in all individuals within 24 h (Fig. 4), and most showed no movement on the appendages. On the other hand, no immediate effects were detected in nauplii treated with KI at 10 mM. After 24 h, no deformities were observed, but some individuals exhibited reduced swimming activity. No significant differences ($p > 0.05$) were observed between the combined TMPyP + KI treatment (under dark or light conditions) and the corresponding treatments with KI alone, indicating that the observed effects were primarily associated with KI rather than photodynamic activity. Considering the inherent toxicity of KI at high concentrations (≥50 mM), the decontamination of brine shrimp nauplii was subsequently evaluated only with TMPyP alone and in combination with KI at the lowest concentration tested (10 mM).

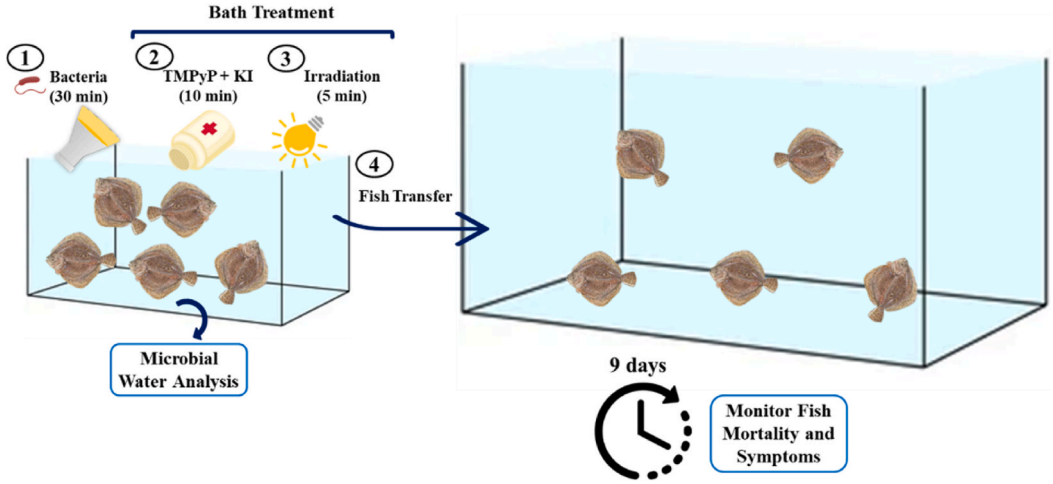

Fig. 2. Representative scheme of aPDI treatment of turbot challenged with *V. anguillarum*.

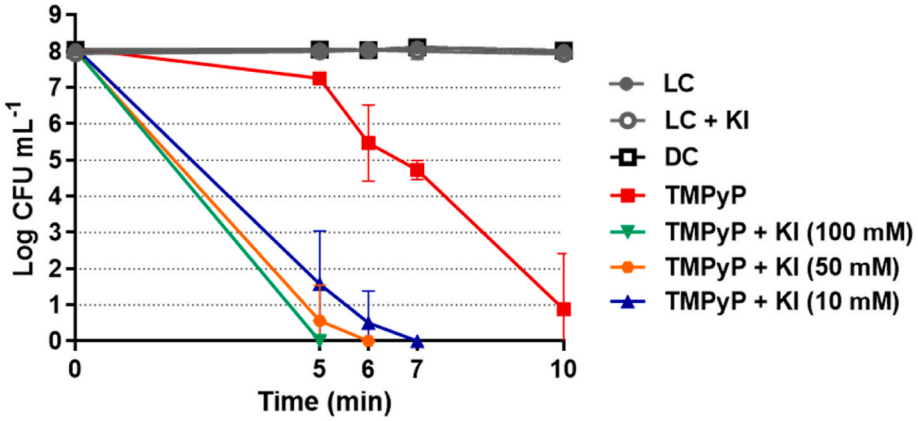

Fig. 3. Photodynamic inactivation of *V. anguillarum* in seawater using TMPyP (5.0 μM), alone and in combination with KI (10, 50, and 100 mM), under 10 min of white light irradiation at an irradiance of 100 mW cm^{-2}. Values represent the mean ± standard deviation of three independent experiments (error bars may be hidden under symbols). LC: light control; DC: dark control.

Table 1
Survival of brine shrimp nauplii immediately after aPDI treatment (short-term toxicity) and 24 h post-treatment (long-term toxicity). Conditions that resulted in mortality rates exceeding 50 % (IC_{50}) are highlighted in red. CT: only brine shrimp nauplii without TMPyP and/or KI.

	Treatments conditions	Survival after treatment (%)	Survival 24 h post-treatment (%)
Irradiated (100 mW cm^{-2})	CT	100 ± 0	100 ± 0
	TMPyP	100 ± 0	100 ± 0
	TMPyP + KI 100 mM	68 ± 9	0
	TMPyP + KI 50 mM	67 ± 9	0
	TMPyP + KI 10 mM	100 ± 0	76 ± 13
	KI 100 mM	69 ± 3	0
	KI 50 mM	72 ± 18	0
	KI 10 mM	100 ± 0	80 ± 20
Protected from light (Dark Controls)	CT	100 ± 0	100 ± 0
	TMPyP	100 ± 0	100 ± 0
	TMPyP + KI 100 mM	85 ± 11	0
	TMPyP + KI 50 mM	82 ± 8	0
	TMPyP + KI 10 mM	100 ± 0	79 ± 14
	KI 100 mM	69 ± 3	0
	KI 50 mM	65 ± 9	0
	KI 10 mM	100 ± 0	85 ± 15

3.2.2. *Photoinactivation of V. anguillarum in brine shrimp*

Before artificial contamination, the presumptive cultivable *Vibrio* spp. counts (assessed on TCBS agar) and the total viable count naturally present in the brine shrimp nauplii were 3.1 and 6.1 log CFU mL^{-1}, respectively (Fig. 5A). Following artificial contamination with *V. anguillarum*, these values increased to 7.4 and 7.8 log CFU mL, respectively. Epifluorescence microscopy confirmed that the internalized *V. anguillarum* was mainly detected in the gut of the brine shrimp nauplii, as shown in Fig. 5B.

Treatments with TMPyP (5.0 μM) alone and in combination with KI (10 mM) were effective in reducing the bacterial concentration in brine shrimp nauplii ($p < 0.05$, Fig. 5C). TMPyP alone caused concentration reductions of 3.1 log CFU mL^{-1} ($p < 0.05$) after 10 min of treatment, reaching a maximum inactivation of 3.8 log CFU mL^{-1} after 60 min. Similar inactivation levels were obtained with TMPyP + KI, indicating that the presence of the salt did not improve the decontamination efficiency under these conditions ($p > 0.05$).

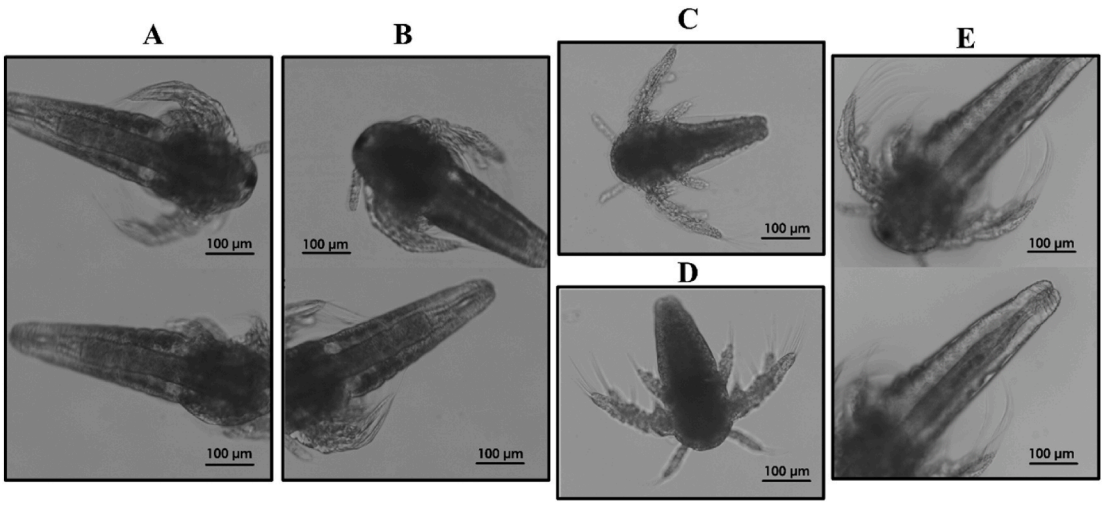

Fig. 4. Photographic images of brine shrimp nauplii taken 24 h after aPDI treatment with TMPyP (5.0 μM) alone (A), TMPyP combined with KI at 10 mM (B) or 100 mM (C), and KI (100 mM) alone (D), under white light irradiation (380-700 nm) for 60 min (100 mW cm^{-2}). A light control (LC; irradiated without PS or KI) was also included (E). These experimental conditions, corresponding to Table 1, are indicated at the top of each image panel. Scale bars = 100 μm.

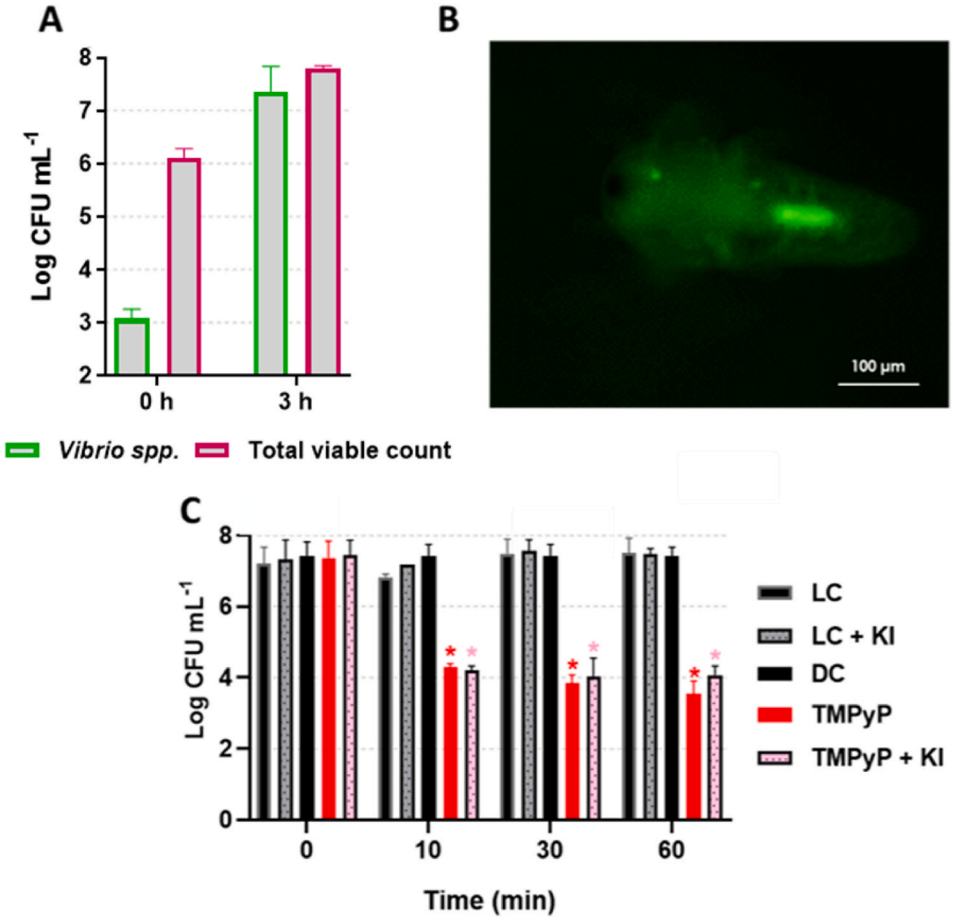

Fig. 5. A) *Vibrio* spp. and total viable counts in brine shrimp nauplii before and after contamination with *V. anguillarum*. B) Detection of fluorescently labelled *V. anguillarum* in brine shrimp nauplii. C) aPDI of *V. anguillarum* in brine shrimp nauplii using TMPyP (5.0 μM), alone and in combination with KI (10 mM), after 10, 30, and 60 min of white light (380-700 nm) irradiation at an irradiance of 100 mW cm^{-2}. Values represent the mean ± standard deviation of three independent experiments (error bars may be hidden under the symbols). LC: light control; DC: dark control. Scale bar = 100 μm. (*) indicates significant ($p < 0.05$, ANOVA) differences in microbial concentration between treated samples and LC.

3.3. Turbot experiments

Preliminary toxicity assays indicated that TMPyP (5.0 μM), alone and in combination with KI at 10 mM, did not cause mortality or behavioural alterations in turbot fingerlings under the conditions tested. On the other hand, its combination with KI at 50 mM proved highly

toxic, leading to approximately 20 % mortality in the dark and 100 % mortality under irradiated conditions. Consequently, the combination of TMPyP (5.0 μM) and KI (10 mM) was selected to evaluate its prophylactic effects against *V. anguillarum* infections in turbot. This combined treatment was the only one tested in the *in vivo* challenge, as it had demonstrated equal or superior effectiveness compared to TMPyP alone in both seawater and brine shrimp decontamination assays.

For these experiments, turbot were immersion-challenged with a lethal concentration of *V. anguillarum* (10^7 CFU mL^{-1}) and, after 30 min of incubation, subjected to a bath treatment with TMPyP and KI (10 min of dark incubation followed by 5 min of irradiation). Water samples were collected before (t = 0 min) and after treatment (t = 5 min) to evaluate the concentration of *V. anguillarum* and the total viable count (Fig. 6A and B). The results revealed that the treatment effectively reduced *Vibrio* concentrations in tank water by 5.5 log CFU mL^{-1} (Fig. 6A). Furthermore, the total viable bacterial count in water was also reduced by 2.8 log CFU mL^{-1} (Fig. 6B).

After treatment, turbot mortality and clinical symptoms were monitored for 9 days. In the non-treated group, mortality reached an average of 70 % within 7 days (Fig. 7), confirming the high virulence of the *V. anguillarum* strain used. Treated fish (Fish_TMPyP + KI_Light) showed a 5 % lower cumulative mortality rate compared to the non-treated controls (Fish), although this difference was not statistically significant ($p > 0.05$).

The analysis of fish symptoms revealed more severe lesions in non-treated fish, including ulcers in the tail and fins, and haemorrhages in abdominal areas (Fig. 8). On the other hand, treated fish displayed milder symptoms (Fig. 8). While most treated fish exhibited tail ulcers and some showed fin lesions, haemorrhages in the abdominal region were rare, no liver bleeding was observed, and some individuals showed no apparent symptoms. Furthermore, dissection revealed the presence of *V. anguillarum* in the fins, tail, and kidneys of non-treated fish; however, the bacterium was not detected in the kidneys of treated fish. Of note, *V. anguillarum* was not detected in the gills of any of the analysed individuals.

4. Discussion

The persistent challenge of vibriosis in farmed turbot, exacerbated by limitations of conventional control methods, highlights the urgent need for innovative antimicrobial strategies [2,3,12–14]. aPDI has emerged as a promising alternative, yet its direct application in aquaculture systems remains largely unexplored [17,18,38,48]. This study, therefore, evaluated the efficacy of TMPyP, alone and in combination with KI, for the decontamination of *V. anguillarum*-contaminated seawater and *Artemia franciscana* nauplii, which are commonly used as live feed in turbot larviculture and constitute a relevant vector for pathogen transmission. In addition, the prophylactic potential of the combined TMPyP + KI treatment was preliminarily assessed in turbot fingerlings pre-challenged with *V. anguillarum*, as a proof-of-concept evaluation under aquaculture-relevant conditions.

4.1. Decontamination of seawater

TMPyP showed significant potential for photoinactivating *V. anguillarum* in natural seawater, achieving a 7.0 log CFU mL^{-1} reduction within 10 min of treatment (Fig. 3). This result aligns with previous findings, where TMPyP under the same conditions produced over a 5.0 log CFU mL^{-1} reduction of *V. anguillarum* in artificial seawater, a matrix designed to simulate the ionic composition of natural seawater [25]. The photodynamic activity of TMPyP has been widely associated with $^1O_2$ generation through a type II aPDI mechanism [49,50]. The efficiency of TMPyP has also been documented against various other *Vibrio* species, including *V. parahaemolyticus*, *V. owensii,* and *V. campbellii* [26,51]. However, in those cases, lower white light intensities (1.2–9.6 mW cm^{-2}) were used, requiring extended irradiation periods (up to 24 h) to achieve comparable levels of disinfection. These findings highlight TMPyP as a versatile PS that can be adapted to various light protocols depending on the intended application. For instance, continuous low-intensity irradiation (1–10 mW cm^{-2}) may be suitable for prophylactic applications and long-term microbial control under standard photoperiod lighting [26,51,52], while high-intensity irradiation (100 mW cm^{-2}) for short periods (5–10 min) enables rapid disinfection.

Over the past decade, the application of KI has been investigated to improve aPDI antimicrobial activity [37,39,53–57]. This synergistic effect has been proposed to rely on the interaction of iodide (I^-) with singlet oxygen ($^1O_2$) generated by the PS during irradiation [37,39,54,57]. This interaction forms hydrogen peroxide (H_2O_2) and reactive iodine species (RIS), including iodine radicals ($I_2^{\bullet-}$) and free iodine/-triiodide (I_2/I_3^-), that are highly bactericidal. In this study, the addition of KI significantly enhanced the photodynamic activity of TMPyP, resulting in bacterial inactivation down to the detection limit of the method (8 log CFU mL^{-1} reduction) with shorter treatment time (Fig. 3). This effect was concentration-dependent, as faster bacterial inactivation was progressively observed at higher KI concentrations (7, 6, and 5 min for 10, 50, and 100 mM KI, respectively). Among the RIS formed, I_2 has been proposed as the primary species responsible for the sustained antimicrobial effect, as previously suggested in our previous study evaluating TMPyP in combination with KI [37]. Its slower decomposition in seawater (with rate constants ranging from 0.030 to 2.31 min^{-1}), compared to the much shorter lifetimes of $^1O_2$, H_2O_2, and $I_2^{\bullet-}$ (<milliseconds), may contribute to its prolonged activity even after irradiation cessation [58,59]. It should be noted, however, that the specific contribution of each RIS to the bactericidal effect observed in the present work was not directly measured, and the mechanistic

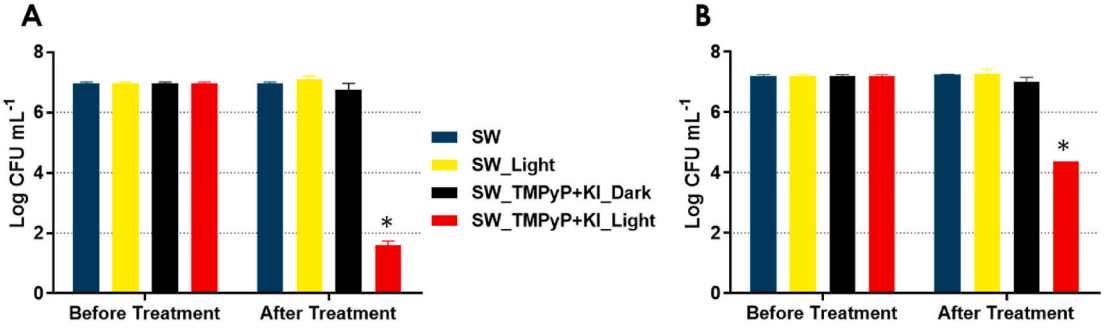

Fig. 6. *V. anguillarum* (A) and total viable counts (B) in seawater from turbot treatment tanks before and after photodynamic treatment with TMPyP (5.0 μM) and KI (10 mM) under 5 min of white light irradiation at an irradiance of 100 mW cm^{-2}. Values represent the mean ± standard deviation of three independent experiments (error bars may be obscured by symbols). SW: seawater; SW_Light: seawater exposed to light only; SW_TMPyP + KI_Dark: seawater treated with TMPyP and KI in the dark; SW_TMPyP + KI_Light: seawater treated with TMPyP and KI under irradiation.

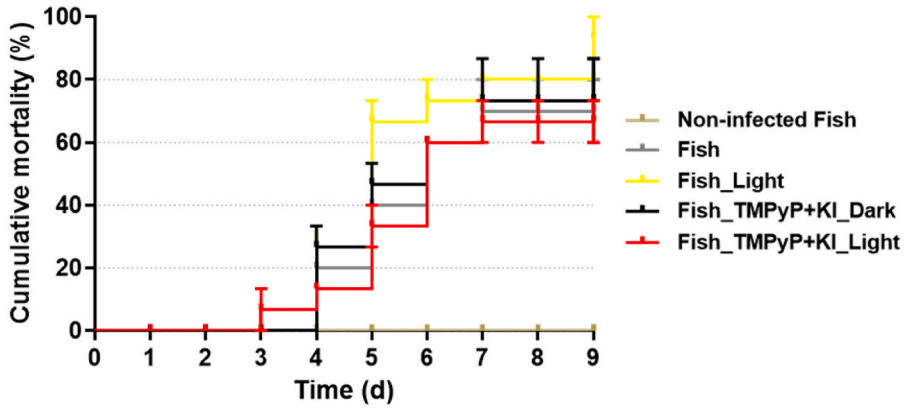

Fig. 7. Cumulative mortality of turbot fingerlings during the 9 days following aPDI treatment. Values represent the mean ± standard deviation of three independent experiments (error bars may be hidden by symbols). Non-infected fish: fish non challenged with *V. anguillarum*; Fish: infected fish; Fish_Light: infected fish exposed to light only; Fish_TMPyP + KI_Dark: infected fish treated with TMPyP and KI in the dark; Fish_TMPyP + KI_Light: infected fish treated with TMPyP and KI under irradiation.

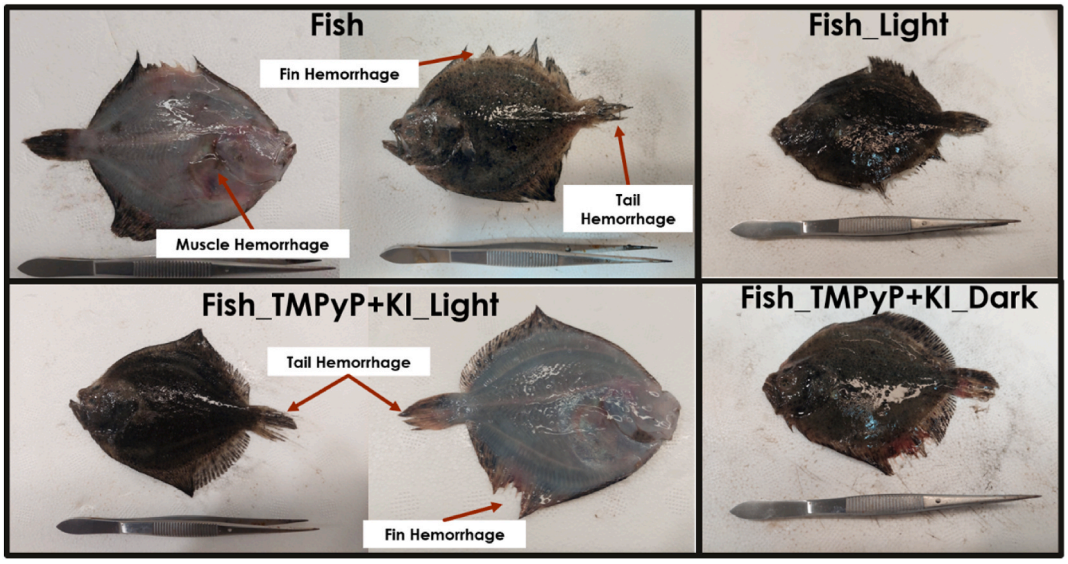

Fig. 8. Clinical signs in juvenile turbot infected with *V. anguillarum*. Fish: infected fish; Fish_Light: infected fish exposed to light only; Fish_TMPyP + KI_Dark: infected fish treated with TMPyP and KI in the dark; Fish_TMPyP + KI_Light: infected fish treated with TMPyP and KI under irradiation.

interpretation provided here is therefore inferred from prior literature rather than experimentally validated in this study. Previous studies have suggested the potential of I_2 generated *in situ* to treat infections *in vivo*, not only by eliminating pathogens, but also preventing their regrowth [40,59]. While this sustained activity may benefit therapeutic applications, it may raise environmental concerns in seawater disinfection. This limitation could be addressed by immobilizing TMPyP and KI on solid supports, enabling their recovery and reuse after treatment. Previous studies have demonstrated effective water and buffer disinfection using polymeric materials containing PS and KI [60,61], supporting future development of reusable TMPyP + KI-based materials for aquaculture applications.

4.2. Decontamination of brine shrimp nauplii

Brine shrimp are a common live food for farmed fish [62,63]. However, they can often become contaminated with *V. anguillarum*, which can infect fish upon ingestion, leading to disease outbreaks [5,6,64]. In aquaculture, brine shrimp cysts are stored for long periods and hatched on demand to provide nauplii for feeding fish [65]. Although decapsulation is primarily performed to improve cyst hatching and handling, the sodium hypochlorite used during this process also reduces the microbial load associated with brine shrimp cysts. However, bacterial regrowth may occur during hatching due to the release of glycerol and other nutrients [62], highlighting the need for decontamination strategies targeting brine shrimp nauplii rather than only cysts. aPDI using TMPyP has been reported to enhance cyst decapsulation and decontamination (reduction of ~5.0 log CFU mL^{-1}; TMPyP at 20 μM, 6 h of white light irradiation at an irradiance of 1.179 mW cm^{-2}) [66]. However, its potential for brine shrimp nauplii decontamination was not assessed. Therefore, in this study, we investigated for the first time the effectiveness of TMPyP, alone and in combination with KI, for brine shrimp decontamination.

The toxicity assays revealed that TMPyP at 5.0 μM was safe for brine shrimp nauplii. However, KI at concentrations of 50 mM or higher caused immediate and long-term harmful effects, including reduced motility, body deformities, and mortality (Fig. 4, Table 1). The toxicity appears to be associated with the KI solution itself rather than I_2, as no significant differences ($p > 0.05$) were observed between treatments with KI alone and TMPyP + KI combinations, regardless of light exposure. This observation is in agreement with previous studies reporting toxic effects of KI compounds in aquatic organisms, including

invertebrates such as *Daphnia magna* and microalgae (*Pseudokirchneriella subcapitata*), with effects dependent on concentration and exposure conditions [67]. Overall, our findings suggest that KI at 10 mM did not cause significant mortality, motility impairment, or morphological alterations in brine shrimp nauplii and can therefore be safely used in combination with TMPyP under the conditions tested. These findings were consistent with the toxicity experiments performed on turbot juveniles, reinforcing that brine shrimp nauplii is a suitable model for preliminary toxicity assessment in aquatic animals [68]. However, it is important to note that further studies evaluating additional toxicity parameters (e.g. growth performance, feeding behavior, histopathology, and gut microbiota composition), as well as other aquatic models such as *D. magna* and zebrafish, are still required to further support the safe application of these treatments in aquaculture.

TMPyP-mediated aPDI was effective at reducing *V. anguillarum* concentration in *A. franciscana* nauplii (>3.0 log CFU mL^{-1}, $p < 0.05$, Fig. 5). These reductions were comparable to natural *Vibrio* loads on brine shrimp nauplii (3.1 log CFU mL^{-1}), highlighting the treatment's potential for decontaminating live food in aquaculture. Under the tested conditions, the application of KI at 10 mM did not improve the treatment efficacy. Similarly, we previously reported that KI did not enhance TMPyP activity during fish fillet decontamination [33], which we tentatively attributed to the low dioxygen availability in biological matriceswhich limits the production of $^1O_2$ and consequently the aPDI-KI synergistic mechanism. However, as this explanation remains hypothetical, further studies should evaluate dioxygen availability in the brine shrimp system. Additionally, the organic molecules present in brine shrimp nauplii may scavenge the $^1O_2$, potentially impacting the production of RIS [69]. The interaction of I_2 with brine shrimp biomolecules, such as unsaturated fats, may also decrease it action [70]. Indeed, *V. anguillarum* was primarily accumulated in the gut of brine shrimp nauplii, an environment where dioxygen levels are known to be very low in other organisms, including aquatic invertebrates [71,72]. Despite this limitation, TMPyP-mediated aPDI showed promising potential for brine shrimp decontamination, especially in comparison with previous studies. In 2012, Asok et al. showed that Rose Bengal (30 μM) reduced *Vibrio harveyi* in brine shrimp nauplii by 91.2 % (1.1 log CFU mL^{-1}) after 30 min of halogen lamp irradiation (450–600 nm) [42]. More recently, Abdulaziz and colleagues (2022) reported that curcumin-mediated aPDI (10 μM) achieved a 68.17 % reduction (0.5 log CFU mL^{-1}) of *Vibrio* spp. in *Penaeus monodon* after 60 min of blue light exposure (λ_{max} 405 nm, 10 mW cm^{-2}) [73]. On the other hand, TMPyP demonstrated higher efficiency, achieving a 99.97 % reduction (3.51 log CFU mL^{-1}) at a lower PS concentration (5.0 μM) with only 10 min of white light irradiation delivered at an irradiance of 100 mW cm^{-2}. Furthermore, TMPyP-mediated aPDI efficiency is comparable to conventional disinfection methods. For instance, previous studies have shown that ozone (O_3), formaldehyde (HCHO) and H_2O_2 led to *Vibrio* reductions of 99.5 % (2.30 log CFU mL^{-1}), 96.0 % (1.40 log CFU mL^{-1}) and 75.8 % (2.30 log CFU mL^{-1}) in brine shrimp nauplii, while sodium hypochlorite (NaOCl) caused bacterial inactivation to the detection limit of the method [74,75]. Nevertheless, it is important to consider that conventional methods often produce toxic by-products and have potential long-term environmental impacts [75–77]. On the other hand, TMPyP can be immobilized onto supports for post-treatment removal, resulting in minimal treatment residues and reduced environmental toxicity [48,78–81]. However, the long-term environmental impacts and possible by-products associated with TMPyP + KI-mediated aPDI were not evaluated in the present study and should be addressed in future investigations.

4.3. Treatment of juvenile turbot

The prophylactic potential of TMPyP + KI mediated aPDI was further assessed in controlling *V. anguillarum* infections in juvenile turbot. Water samples collected from the turbot tanks showed that this treatment effectively reduced *V. anguillarum* levels (5.5 log CFU mL^{-1}, Fig. 6). In contrast, the reduction observed for total viable counts was comparatively lower (2.8 log CFU mL^{-1}), suggesting a more selective effect on *V. anguillarum* compared to the natural microbiota of seawater. These findings align with previous studies describing that *Vibrio* species are generally more susceptible to aPDI than other Gram-negative bacteria [25,28,82–84]. The increased susceptibility of *Vibrio* species has been proposed to be related to their outer membrane composition, particularly a higher content of polyunsaturated fatty acids that are more prone to oxidative damage by $^1O_2$ [25,85,86].

Although aPDI efficiently photoinactivated *V. anguillarum* in seawater, the treatment did not significantly reduce turbot mortality (Fig. 7). This may be attributed to the 30-min bacterial exposure period before treatment, during which the infection could have already been initiated. A previous study showed that immersion of striped catfish (*Pangasianodon hypophthalmus*) in a suspension of *Edwardsiella ictaluri* for only 30 s was sufficient to establish infection [87]. Therefore, *V. anguillarum* may have adhered to the skin or entered through the gastrointestinal tract before aPDI was applied. In contrast, the gills appear less likely to be a route of entry, since no bacteria were detected in this tissue. These findings highlight the importance of optimizing treatment timing and suggest that aPDI may be effective when applied at earlier stages of exposure.

aPDI has previously been shown to reduce bacterial concentration on fish skin [33], however, complete pathogen elimination is challenging due to the presence of organic matter and the complex structure of the skin surface [88]. In addition, the limited light penetration through the turbot's dark and opaque skin may have reduced the effectiveness of aPDI in targeting internal tissue, similar to what has been observed in other tissues [89]. Although mortality was not significantly reduced, treated fish displayed milder clinical symptoms, including fewer external haemorrhages and an absence of abdominal haemorrhages (Figs. 7 and 8), suggesting a partial protective effect. These findings suggest that the potential of PDI in aquaculture mainly lies in the preventive decontamination of the aquaculture environment, while its application in the treatment of fish infections requires further investigation.

The antimicrobial effect of aPDI treatment may have contributed to limiting infection severity. Notably, *V. anguillarum* was not detected in the kidneys of treated fish, suggesting the restriction of infection progression. Similarly, Wong et al. (2005) reported that Toluidine Blue O-mediated aPDI suppressed protease activity and reduced the severity of septicaemia caused by *Vibrio vulnificus* in mice, an effect associated with suppression of bacterial motility and protease secretion [90]. More recently, Bartolomeu et al. (2016) demonstrated that irradiated TMPyP damaged *Staphylococcus aureus* enterotoxins and altered the expression of functional proteins, although it remains unclear whether such changes persist across bacterial generations [41]. It is therefore possible that in the present study, aPDI may have contributed to reducing *V. anguillarum* virulence by damaging and/or suppressing the expression of proteins critical to pathogenesis, such as adhesins, outer membrane proteins, and proteases. It could also result in a lower production of hemolysins, exotoxins responsible for erythrocyte lysis and haemorrhage [4]. These antimicrobial effects may have been complemented by the wound-healing properties of aPDI. Prior studies have shown that aPDI can reduce inflammation and enhance tissue repair by modulating molecular, pathological, and bactericidal processes [91,92]. These mechanistic considerations remain, however, hypothetical and are not directly demonstrated by the *in vivo* data presented here.

Nevertheless, even with attenuated virulence, colonization can still trigger the host's innate and adaptive immune responses [93–95]. Excessive production of inflammatory mediators may lead to systemic inflammatory response syndrome or septic shock [4], ultimately causing death in both treated and untreated groups. To fully understand *V. anguillarum* infection in turbot and the potential beneficial effects of TMPyP + KI-mediated aPDI, further research should evaluate the impact

of treatment on bacterial virulence factors and the host immune response. Exploring a wider range of TMPyP concentrations and irradiation doses may also help optimize treatment efficacy. Future studies should explore the potential of TMPyP + KI-mediated PDI for preventing infections in turbot larvae. This life stage is not only more susceptible to vibriosis [96] but also potentially more responsive to aPDI, as larvae are smaller, less pigmented, and more permeable to light, which may allow PDI to target deeper tissues more effectively.

Since the *in vivo* turbot assays were designed as a proof-of-concept evaluation under aquaculture-relevant conditions and in accordance with the 3Rs principle [97], TMPyP-alone and KI-alone irradiated control groups were not included, in order to minimize the number of animals subjected to experimental procedures. Consequently, the individual contribution of TMPyP and any synergistic effect with KI could not be directly assessed *in vivo* in the present study and were inferred from the *in vitro* results and from previous literature. Future studies, designed within appropriate ethical boundaries, should include such control groups to determine the individual contribution of each component and to assess potential synergistic effects under *in vivo* conditions.

To the best of our knowledge, only one study has evaluated the potential of aPDI to treat bacterial infections in fish. In 2024, Liu et al. reported that TTCPy-3, an aggregation-induced emission PS, was effective in treating zebrafish infected with *Nocardia seriolae*, a Gram-positive bacterium [32]. TTCPy-3 at 10 μM reduced bacterial dissemination and improved survival rates from 30.95 to 95.24 %. However, even without irradiation, TTCPy-3 treatment decreased mortality to 82.54 %, suggesting that its antimicrobial activity may not be solely attributed to aPDI but could involve additional antimicrobial mechanisms.

5. Conclusion

In this study, TMPyP, both alone and in combination with KI, showed promising results for decontaminating seawater and brine shrimp nauplii artificially contaminated with *V. anguillarum*. The combined treatment was more effective in reducing *V. anguillarum* levels in seawater compared to TMPyP alone. However, the addition of KI did not significantly enhance the treatment's effectiveness in brine shrimp. In the *in vivo* turbot model, the tested PDI protocol did not significantly reduce mortality; however, treated animals showed milder clinical signs, suggesting a potential partial prophylactic effect that merits further investigation. Overall, our findings suggest that aPDI mediated by TMPyP, alone or combined with KI, is a promising strategy for mitigating *V. anguillarum* contamination in aquaculture by reducing microbial loads in seawater and in live food, with potential value as a prophylactic tool rather than as a curative intervention for already established infections. Future studies should focus on optimizing aPDI protocols, particularly with regard to treatment timing, dose, exposure regimen, and integration into routine aquaculture practices, to better assess their prophylactic potential and to clarify the mechanisms underlying the protective effects observed *in vivo*.

Ethical approval

All experimental protocols involving fish were carried out in accordance with European and Spanish legislation for the use of animals for scientific purposes (Directive 2010/63/EU) and were approved by Bioethics Committee of the University of Santiago de Compostela (Protocol N° 15012/2022/001).

Funding

This research was supported by the University of Aveiro and FCT/MECI (Fundação para a Ciência e a Tecnologia and Ministério da Educação, Ciência e Inovação) through the financial support of UID Centro de Estudos do Ambiente e Mar (CESAM), references UID/50017/2025 (doi.org/10.54499/UID/50017/2025) and LA/P/0094/2020 (doi.org/10.54499/LA/P/0094/2020) and the UID/50006 LAQV-REQUIMTE—Laboratório Associado para a Química Verde—Tecnologias e Processos Limpos (doi: 10.54499/UID/50006/2025), and to project PREVINE—FCT-PTDC/ASP-PES/29576/2017), through the financial support of the Centre for Interdisciplinary Research in Health (CIIS) under the Strategic Project Nos. UIDB/04279/2020 and UIDP/04279/2020, through national funds (OE) and, where applicable, was co-financed by the FEDER-Operational Thematic Program for Competitiveness and Internationalization-COMPETE 2020, within the PT2020 Partnership Agreement funded by national funds. This work was also supported by grant ED431C2022/23 from Xunta de Galicia (Spain).

CRediT authorship contribution statement

Cátia Vieira: Conceptualization, Data curation, Formal analysis, Investigation, Methodology, Visualization, Writing – original draft, Writing – review & editing. **Maria Bartolomeu:** Validation, Writing – review & editing. **Pedro P. Gallego:** Supervision, Writing – review & editing. **M. Graça P.M. S. Neves:** Supervision, Writing – review & editing. **Jesús L. Romalde:** Conceptualization, Funding acquisition, Investigation, Methodology, Project administration, Resources, Supervision, Validation, Writing – review & editing. **M. Amparo F. Faustino:** Funding acquisition, Project administration, Resources, Supervision, Validation, Writing – review & editing. **Adelaide Almeida:** Conceptualization, Funding acquisition, Project administration, Resources, Supervision, Validation, Writing – review & editing.

Declaration of competing interest

The authors declare that they have no known competing financial interests or personal relationships that could have appeared to influence the work reported in this paper.

Acknowledgments

The authors thank the University of Aveiro and FCT/MECI for financial support to the UID Centro de Estudos do Ambiente e Mar (CESAM) + LA/P/0094/2020 the UID/50006 LAQV-REQUIMTE—Laboratório Associado para a Química Verde—Tecnologias e Processos Limpos, and to project PREVINE (FCT-PTDC/ASP-PES/29576/2017), through national funds (OE) and where applicable co-financed by the FEDER-Operational Thematic Program for Competitiveness and Internationalization-COMPETE 2020, within the PT2020 Partnership Agreement. Cátia Vieira (C.V.) thanks FCT for her Ph.D grant (SFRH/BD/150358/2019).

Authors acknowledge the staff of the Aquarium facilities for their help in the maintenance of the fishes.

Data availability

Data will be made available on request.

References

[1] Mohamad N, Amal MNA, Yasin ISM, Zamri Saad M, Nasruddin NS, Al-saari N, Mino S, Sawabe T. Vibriosis in cultured marine fishes: a review. Aquaculture 2019; 512:734289. https://doi.org/10.1016/j.aquaculture.2019.734289.

[2] Hickey ME, Lee J-L. A comprehensive review of Vibrio (Listonella) anguillarum: ecology, pathology and prevention. Rev Aquac 2018;10:585–610. https://doi.org/10.1111/raq.12188.

[3] Gao Y, Wang Q, Liu Y, Ma Y, Jin H, Liu J, Wang H, Yan Y, Li J. Epidemiology of turbot bacterial diseases in China between October 2016 and December 2019. Front Mar Sci 2023;10. https://doi.org/10.3389/fmars.2023.1145083. 2023.

[4] Frans I, Michiels CW, Bossier P, Willems KA, Lievens B, Rediers H. Vibrio anguillarum as a fish pathogen: virulence factors, diagnosis and prevention. J Fish Dis 2011;34:643–61. https://doi.org/10.1111/j.1365-2761.2011.01279.x.

[5] Grisez L, Sorgeloos P, Ollevier F. Mode of infection and spread of Vibrio anguillarum in turbot Scophthalmus maximus larvae after oral challenge through live feed. Dis Aquat Organ 1996;26:181–7. https://api.semanticscholar.org/CorpusID:59426906.

[6] Kumaran T, Citarasu T. Characterization of Vibrio Species from shrimp and artemia culture and evaluation of the potential virulence factor. Intellect Prop Rights 2016;4:1–5. https://doi.org/10.4172/2375-4516.1000153.

[7] Xu K, Wang Y, Yang W, Cai H, Zhang Y, Huang L. Strategies for prevention and control of vibriosis in Asian fish culture. Vaccines 2022;11. https://doi.org/10.3390/vaccines11010098.

[8] Kumar A, Middha SK, Menon SV, Paital B, Gokarn S, Nelli M, Rajanikanth RB, Chandra HM, Mugunthan SP, Kantwa SM, Usha T, Hati AK, Venkatesan D, Rajendran A, Behera TR, Venkatesamurthy S, Sahoo DK. Current challenges of vaccination in fish health management. Animals 2024;14:2692. https://doi.org/10.3390/ani14182692.

[9] Parin U, Erbas G, Savasan S, Yuksel HT, Gurpinar S, Kirkan S. Antimicrobial resistance of Vibrio (Listonella) anguillarum isolated from rainbow trouts (Oncorhynchus mykiss). Agric Res Commun Cent 2019;53:1522–5. https://doi.org/10.18805/ijar.v0iOF.7251.

[10] Cherian T, Ragavendran C, Vijayan S, Kurien S, Peijnenburg WJGM. A review on the fate, human health and environmental impacts, as well as regulation of antibiotics used in aquaculture. Environ Adv 2023;13:100411. https://doi.org/10.1016/j.envadv.2023.100411.

[11] Rurangwa E, Verdegem MCJ. Microorganisms in recirculating aquaculture systems and their management. Rev Aquac 2015;7:117–30. https://doi.org/10.1111/raq.12057.

[12] Jensen MA, Ritar AJ, Burke C, Ward LR. Seawater ozonation and formalin disinfection for the larval culture of eastern rock lobster, Jasus (Sagmariasus) verreauxi, phyllosoma. Aquaculture 2011;318:213–22. https://doi.org/10.1016/j.aquaculture.2011.05.001.

[13] Xin L, Youping S, Lihong Q. Marine ecological impact analysis of residual chlorine emission from LNG transfer station. E3S Web Conf 2023;393. https://doi.org/10.1051/e3sconf/202339302009.

[14] Shibai A, Takahashi Y, Ishizawa Y, Motooka D, Nakamura S, Ying B-W, Tsuru S. Mutation accumulation under UV radiation in Escherichia coli. Sci Rep 2017;7:14531. https://doi.org/10.1038/s41598-017-15008-1.

[15] Bartolomeu M, Gomes TJ, Campos F, Vieira C, Loureiro S, Neves MGPMS, Faustino MAF, Gomes ATPC, Almeida A. Wastewater disinfection with photodynamic treatment and evaluation of its ecotoxicological effects. Chemosphere 2024;361:142421. https://doi.org/10.1016/j.chemosphere.2024.142421.

[16] Mendonça I, Silva D, Conde T, Maurício T, Cardoso H, Pereira H, Bartolomeu M, Vieira C, Domingues MR, Almeida A. Insight into the efficiency of microalgae' lipidic extracts as photosensitizers for Antimicrobial Photodynamic Therapy against Staphylococcus aureus. J Photochem Photobiol B Biol 2024;259:112997. https://doi.org/10.1016/j.jphotobiol.2024.112997.

[17] Pucelik B, Dąbrowski JM. Chapter three - photodynamic inactivation (PDI) as a promising alternative to current pharmaceuticals for the treatment of resistant microorganisms. In: van Eldik R, Hubbard CD, editors. Recent highlights II. Academic Press; 2022. p. 65–108. https://doi.org/10.1016/bs.adioch.2021.12.003.

[18] Vieira C, Santos A, Mesquita MQ, Gomes ATPC, Neves GPMS, Faustino AF, Adelaide A. Advances in aPDT based on the combination of a porphyrinic formulation with potassium iodide: effectiveness on bacteria and fungi planktonic/biofilm forms and viruses. J Porphyr Phthalocyanines 2019;23:534–45. https://doi.org/10.1142/S1088424619500408.

[19] Costa LD, Vieira C, Hackbarth S, Neves MGPMS, Almeida A, Faustino MAF, Tomé AC. Photodynamic inactivation of Escherichia coli and Staphylococcus aureus by cationic diketopyrrolopyrroles. Dye Pigment 2026;244:113101. https://doi.org/10.1016/j.dyepig.2025.113101.

[20] Jori G, Camerin M, Soncin M, Guidolin L, Coppellotti O. Antimicrobial photodynamic therapy: basic principles. R Soc Chem 2011:1–18. http://pubs.rsc.org/en/content/chapter/bk9781849731447-00001/978-1-84973-144-7/unauth.

[21] Cieplik F, Deng D, Crielaard W, Buchalla W, Hellwig E, Al-Ahmad A, Maisch T. Antimicrobial photodynamic therapy–what we know and what we don't. Crit Rev Microbiol 2018;44:571–89. https://doi.org/10.1080/1040841X.2018.1467876.

[22] Reis MJA, Vieira C, Bartolomeu M, Faustino MAF, Pereira AMVM, Neves MGPMS, Almeida A, Moura NMM. A2B2-type porphyrins enhanced by N-donor units: synthesis optimization and photodynamic efficiency towards S. aureus. Bioorg Chem 2025;162:108607. https://doi.org/10.1016/j.bioorg.2025.108607.

[23] Alves E, Santos N, Melo T, Maciel E, Dória ML, Faustino MAF, Tomé JPC, Neves MGPMS, Cavaleiro JAS, Cunha Â, Helguero LA, Domingues P, Almeida A, Domingues MRM. Photodynamic oxidation of Escherichia coli membrane phospholipids: new insights based on lipidomics. Rapid Commun Mass Spectrom 2013;27:2717–28. https://doi.org/10.1002/rcm.6739.

[24] Alves E, Moreirinha C, Faustino MAF, Cunha Â, Delgadillo I, Neves MG, Almeida A. Overall biochemical changes in bacteria photosensitized with cationic porphyrins monitored by infrared spectroscopy. Future Med Chem 2016;8:613–28. https://doi.org/10.4155/fmc-2015-0008.

[25] Vieira C, Bartolomeu M, Monteiro CJP, Romalde JL, Gallego PP, Neves MGPMS, Faustino MAF, Almeida A. Cationic photosensitizers and potassium iodide: an innovative approach for enhanced photodynamic inactivation of pathogenic bacteria in aquaculture. Aquaculture 2025;596:741882. https://doi.org/10.1016/j.aquaculture.2024.741882.

[26] Malara D, Mielke C, Oelgemöller M, Senge MO, Heimann K. Sustainable water treatment in aquaculture – photolysis and photodynamic therapy for the inactivation of Vibrio species. Aquac Res 2017;48:2954–62. https://doi.org/10.1111/are.13128.

[27] Alves E, Faustino MAF, Tomé JPC, Neves MGPMS, Tomé AC, Cavaleiro JAS, Cunha Â, Gomes NCM, Almeida A. Photodynamic antimicrobial chemotherapy in aquaculture: photoinactivation studies of Vibrio fischeri. PLoS One 2011;6:1–9. https://doi.org/10.1371/journal.pone.0020970.

[28] Arrojado C, Pereira C, Tomé JP, Faustino MAF, Neves MGPMS, Tomé AC, Cavaleiro JASS, Cunha Â, Calado R, Gomes NC, Almeida A. Applicability of photodynamic antimicrobial chemotherapy as an alternative to inactivate fish pathogenic bacteria in aquaculture systems. Photochem Photobiol Sci 2011;10:1691–700. https://doi.org/10.1039/C1PP05129F.

[29] Dube E, Okuthe GE. Applications of antimicrobial photodynamic therapy in aquaculture: effect on fish pathogenic bacteria. Fishes 2024;9:99. https://doi.org/10.3390/fishes9030099.

[30] Mantareva V, Kussovski V, Orozova P, Angelov I, Durmuş M, Najdenski H. Palladium phthalocyanines varying in substituents position for photodynamic inactivation of Flavobacterium hydatis as sensitive and resistant species. Curr Issues Mol Biol 2022;44:1950–9. https://doi.org/10.3390/cimb44050133.

[31] Magaraggia M, Faccenda F, Gandolfi A, Jori G. Treatment of microbiologically polluted aquaculture waters by a novel photochemical technique of potentially low environmental impact. J Environ Monit 2006;8:923–31. https://doi.org/10.1039/b606975d.

[32] Liu Z, Zhang J, Ma X, Wang M, Jiang L, Zhang M, Lu M, Chang O, Cao J, Ke X, Yi M. Aggregation-induced emission of TTCPy-3: a novel approach for eradicating Nocardia seriolae infections in aquatic fishes. Biosens Bioelectron 2024;254:116208. https://doi.org/10.1016/j.bios.2024.116208.

[33] Vieira C, Trigo M, Dias CJ, Bartolomeu M, Gallego PP, Neves MGPMS, Iglesias R, Aubourg SP, Faustino MAF, Almeida A. Photodynamic inactivation as a novel approach for seabass decontamination: effectiveness of TMPyP and methylene blue treatments. Food Bioprocess Technol 2025;18:7112–30. https://doi.org/10.1007/s11947-025-03869-8.

[34] Simões C, Gomes MC, Neves MGPMS, Cunha Â, Tomé JPC, Tomé AC, Cavaleiro JAS, Almeida A, Faustino MAF. Photodynamic inactivation of Escherichia coli with cationic meso-tetraarylporphyrins - the charge number and charge distribution effects. Catal Today 2016;266:197–204. https://doi.org/10.1016/j.cattod.2015.07.031.

[35] Sorgeloos P, Bossuyt E, Laviña E, Baeza-Mesa M, Persoone G. Decapsulation of Artemia cysts: a simple technique for the improvement of the use of brine shrimp in aquaculture. Aquaculture 1977;12:311–5. https://doi.org/10.1016/0044-8486(77)90209-5.

[36] Bartolomeu M, Vieira C, Dias M, Conde T, Couto D, Lopes D, Neves B, Melo T, Rey F, Alves E, Silva J, Abreu H, Almeida A, Domingues MR. Bioprospecting antibiotic properties in photodynamic therapy of lipids from codium tomemtosum and Chlorella vulgaris. Biochimie 2022;203:32–9. https://doi.org/10.1016/j.biochi.2022.09.012.

[37] Vieira C, Gomes ATPC, Mesquita MQ, Moura NMM, Neves MGPMS, Faustino MAF, Almeida A. An insight into the potentiation effect of potassium iodide on aPDT efficacy. Front Microbiol 2018;9:1–16. https://doi.org/10.3389/fmicb.2018.02665.

[38] Chaves I, Morais FMP, Vieira C, Bartolomeu M, Faustino MAF, Neves MGPMS, Almeida A, Moura NMM. Can porphyrin–triphenylphosphonium conjugates enhance the photosensitizer performance toward bacterial strains? ACS Appl Bio Mater 2024;7:5541–52. https://doi.org/10.1021/acsabm.4c00659.

[39] Vecchio D, Gupta A, Huang L, Landi G, Avci P, Rodas A, Hamblina MR. Bacterial photodynamic inactivation mediated by methylene blue and red light is enhanced by synergistic effect of potassium iodide. Antimicrob Agents Chemother 2015;59:5203–12. https://doi.org/10.1128/AAC.00019-15.

[40] Huang L, Szewczyk G, Sarna T, Hamblin MR. Potassium iodide potentiates broad-spectrum antimicrobial photodynamic inactivation using photofrin. ACS Infect Dis 2017;3:320–8. https://doi.org/10.1021/acsinfecdis.7b00004.

[41] Bartolomeu M, Rocha S, Cunha Â, Neves MGPMS, Faustino MAF, Almeida A. Effect of photodynamic therapy on the virulence factors of Staphylococcus aureus. Front Microbiol 2016;7:267. https://doi.org/10.3389/fmicb.2016.00267.

[42] Asok A, Arshad E, Jasmin C, Pai SS, Singh ISB, Mohandas A, Anas A. Reducing Vibrio load in Artemia nauplii using antimicrobial photodynamic therapy: a promising strategy to reduce antibiotic application in shrimp larviculture. Microb Biotechnol 2012;5:59–68. https://doi.org/10.1111/j.1751-7915.2011.00297.x.

[43] Sahandi J, Sorgeloos P, Zhang W. Culture of Artemia franciscana nauplii with selected microbes suppressed Vibrio loading and enhanced survival, population stability, enzyme activity, and chemical composition. Aquac Int 2022;30:2279–93. https://doi.org/10.1007/s10499-022-00905-8.

[44] Kronvall G, Myhre E. Differential staining of bacteria in clinical specimens using acridine orange buffered at low pH. Acta Pathol Microbiol Scand Sect B Microbiol 1977;85B:249–54. https://doi.org/10.1111/j.1699-0463.1977.tb01970.x.

[45] Ramirez M, Domínguez-Borbor C, Salazar L, Debut A, Vizuete K, Sonnenholzner S, Alexis F, Rodríguez J. The probiotics Vibrio diabolicus (Ili), Vibrio hepatarius (P62), and Bacillus cereus sensu stricto (P64) colonize internal and external surfaces of Penaeus vannamei shrimp larvae and protect it against Vibrio parahaemolyticus. Aquaculture 2022;549:737826. https://doi.org/10.1016/j.aquaculture.2021.737826.

[46] Costa P, Pereira C, Barja JL, Romalde JL, Almeida A. Enhancing bivalve depuration using a phage cocktail: an in vitro and in vivo study. Food Control 2025;177:111442. https://doi.org/10.1016/j.foodcont.2025.111442.

[47] Isidan H, Ozturk RC, Aydin I. Effect of ploidy status of juvenile turbot , Scophthalmus maximus , on innate immune response and disease susceptibility

against Aeromonas salmonicida , Vibrio anguillarum and Viral hemorrhagic septicemia virus. Bull Eur Assoc Fish Pathol 2022;41:1–17.
[48] Mesquita MQ, Dias CJ, Neves MGPMS, Almeida A, Faustino MAF. Revisiting current photoactive materials for antimicrobial photodynamic therapy. Molecules 2018;23:2424. https://doi.org/10.3390/molecules23102424.
[49] Wilkinson F, Helman WP, Ross AB. Quantum yields for the photosensitized formation of the lowest electronically excited singlet state of molecular oxygen in solution. J Phys Chem Ref Data 1993;22:113–262. https://doi.org/10.1063/1.555934.
[50] Tavares A, Dias SRS, Carvalho CMB, Faustino MAF, Tomé JPC, Neves MGPMS, Tomé AC, Cavaleiro JAS, Cunha Â, Gomes NCM, Alves E, Almeida A. Mechanisms of photodynamic inactivation of a Gram-negative recombinant bioluminescent bacterium by cationic porphyrins. Photochem Photobiol Sci 2011;10:1659–69. https://doi.org/10.1039/c1pp05097d.
[51] Malara D, Hoj L, Heimann K, Citarrella G, Oelgemöller M. Capacity of cationic and anionic porphyrins to inactivate the potential aquaculture pathogen Vibrio campbellii. Aquaculture 2017;473:228–36. https://doi.org/10.1016/j.aquaculture.2017.02.015.
[52] Costa L, Carvalho CMB, Faustino MAF, Neves MGPMS, Tomé JPC, Tomé AC, Cavaleiro JAS, Cunha Â, Almeida A. Sewage bacteriophage inactivation by cationic porphyrins: influence of light parameters. Photochem Photobiol Sci 2010;9:1126–33. https://doi.org/10.1039/c0pp00051e.
[53] Zhang Y, Dai T, Wang M, Vecchio D, Chiang LY, Hamblin MR. Potentiation of antimicrobial photodynamic inactivation mediated by a cationic fullerene by added iodide: in vitro and in vivo studies. Nanomedicine 2015;10:603–14. https://doi.org/10.2217/nnm.14.131.
[54] Hamblin MR. Potentiation of antimicrobial photodynamic inactivation by inorganic salts. Expert Rev Anti Infect Ther 2017;15:1059–69. https://doi.org/10.1080/14787210.2017.1397512.
[55] Gamelas SRD, Bartolomeu M, Vieira C, Faustino MAF, Tomé JPC, Tomé AC, Almeida A, Lourenço LMO. Bacterial photodynamic inactivation: eradication of Staphylococcus aureus and Escherichia coli mediated by pyridinium-pyrazolyl Zinc (II) phthalocyanines. ACS Appl Bio Mater 2024;7:7748–57. https://doi.org/10.1021/acsabm.4c01368.
[56] Sarabando SN, Dias CJ, Vieira C, Bartolomeu M, Neves MGPMS, Almeida A, Monteiro CJP, Faustino MAF. Sulfonamide porphyrins as potent photosensitizers against multidrug-resistant Staphylococcus aureus (MRSA): the role of Co-Adjuvants. Molecules 2023;28:2067. https://doi.org/10.3390/molecules28052067.
[57] Kashef N, Huang YY, Hamblin MR. Advances in antimicrobial photodynamic inactivation at the nanoscale. Nanophotonics 2017;6:853–79. https://doi.org/10.1515/nanoph-2016-0189.
[58] Truesdale VW. The chemical reduction of molecular iodine added to seawater, modelled as a system of linked first-order reactions. Mar Chem 1993;42:147–66. https://doi.org/10.1016/0304-4203(93)90009-D.
[59] Wen X, Zhang X, Szewczyk G, El-Hussein A, Huang Y-YY, Sarna T, Hamblin MR. Potassium iodide potentiates antimicrobial photodynamic inactivation mediated by rose bengal in in vitro and in vivo studies. Antimicrob Agents Chemother 2017;61. https://doi.org/10.1128/AAC.00467-17. 10.1128/aac.00467-17.
[60] López-Fernández AM, Moisescu EE, de Llanos R, Galindo F. Development of a polymeric film entrapping rose bengal and iodide anion for the light-induced generation and release of bactericidal hydrogen peroxide. Int J Mol Sci 2022;23. https://doi.org/10.3390/ijms231710162.
[61] Ekka A, Gupta V. Assessment of bacterial photodynamic inactivation mediated by methylene blue in the presence of potassium iodide. J Popul Ther Clin Pharmacol 2022;29:1470–9. https://doi.org/10.53555/jptcp.v29i04.4482.
[62] Sorgeloos P, Dhert P, Candreva P. Use of the brine shrimp, Artemia spp., in marine fish larviculture. Aquaculture 2001;200:147–59. https://doi.org/10.1016/S0044-8486(01)00698-6.
[63] Abate TG, Nielsen R, Nielsen M, Jepsen PM, Hansen BW. A cost-effectiveness analysis of live feeds in juvenile turbot Scophthalmus maximus (Linnaeus, 1758) farming: copepods versus Artemia. Aquac Nutr 2016;22:899–910. https://doi.org/10.1111/anu.12307.
[64] Quiroz-Guzmán E, Balcázar JL, Vázquez-Juárez R, Cruz-Villacorta AA, Martínez-Díaz SF. Proliferation, colonization, and detrimental effects of Vibrio parahaemolyticus and Vibrio harveyi during brine shrimp hatching. Aquaculture 2013;406–407:85–90. https://doi.org/10.1016/j.aquaculture.2013.03.008.
[65] Madkour K, Dawood MAO, Sewilam H. The use of artemia for aquaculture industry: an updated overview. Ann Anim Sci 2023;23:3–10. https://doi.org/10.2478/aoas-2022-0041.
[66] Malara D. Photodynamic antimicrobial chemotherapy for pathogenic vibrio control in prawn hatcheries. James Cook University; 2017. https://doi.org/10.25903/5bac064fe5557.
[67] Mori IC, Arias-Barreiro CR, Koutsaftis A, Ogo A, Kawano T, Yoshizuka K, Inayat-Hussain SH, Aoyama I. Toxicity of tetramethylammonium hydroxide to aquatic organisms and its synergistic action with potassium iodide. Chemosphere 2015;120:299–304. https://doi.org/10.1016/j.chemosphere.2014.07.011.
[68] Yu J, Lu Y. Artemia spp. model - a well-established method for rapidly assessing the toxicity on an environmental perspective. Med Res Arch 2018;6:1–15.
[69] Romera-Castillo C, Jaffé R. Free radical scavenging (antioxidant activity) of natural dissolved organic matter. Mar Chem 2015;177:668–76. https://doi.org/10.1016/j.marchem.2015.10.008.
[70] Apostolov K. The effects of iodine on the biological activities of myxoviruses. J Hyg 1980;84:381–8. https://doi.org/10.1017/s0022172400026905.
[71] Singhal R, Shah YM. Oxygen battle in the gut: hypoxia and hypoxia-inducible factors in metabolic and inflammatory responses in the intestine. J Biol Chem 2020;295:10493–505. https://doi.org/10.1074/jbc.REV120.011188.
[72] Gross EM, Brune A, Walenciak O. Gut pH, redox conditions and oxygen levels in an aquatic caterpillar: potential effects on the fate of ingested tannins. J Insect Physiol 2008;54:462–71. https://doi.org/10.1016/j.jinsphys.2007.11.005.
[73] Abdulaziz A, Pramodh AV, Sukumaran V, Raj D, John AMVB. The influence of photodynamic antimicrobial chemotherapy on the microbiome, neuroendocrine and immune System of Crustacean Post Larvae. Toxics 2022;11:36. https://doi.org/10.3390/toxics11010036.
[74] Tolomei A, Burke C, Crear B, Carson J. Bacterial decontamination of on-grown Artemia. Aquaculture 2004;232:357–71. https://doi.org/10.1016/S0044-8486(03)00540-4.
[75] Sun X, Yang C, Zhang W, Zheng J, Ou J, Ou S. Toxicity of formaldehyde, and its role in the formation of harmful and aromatic compounds during food processing. Food Chem X 2025;25:102225. https://doi.org/10.1016/j.fochx.2025.102225.
[76] Simpson AMA, Mitch WA. Chlorine and ozone disinfection and disinfection byproducts in postharvest food processing facilities: a review. Crit Rev Environ Sci Technol 2022;52:1825–67. https://doi.org/10.1080/10643389.2020.1862562.
[77] Affrald RJ. Sodium hypochlorite and its environmental impacts ; time to switch for herbal alternatives. Toxicol Int 2022;29:215–26. https://doi.org/10.18311/ti/2022/v29i2/29010.
[78] Gamito G, Monteiro CJ, Dias MC, Oliveira H, Silva AM, Faustino MAF, Silva S. Impact of Fe(3)O(4)-porphyrin hybrid nanoparticles on wheat: physiological and metabolic advance. J Hazard Mater 2024;471:134243. https://doi.org/10.1016/j.jhazmat.2024.134243.
[79] Alves E, Rodrigues JMM, Faustino MAF, Neves MGPMS, Cavaleiro JAS, Lin Z, Cunha Â, Nadais MH, Tomé JPC, Almeida A. A new insight on nanomagnet–porphyrin hybrids for photodynamic inactivation of microorganisms. Dye Pigment 2014;110:80–8. https://doi.org/10.1016/j.dyepig.2014.05.016.
[80] Castro KA, Moura NM, Fernandes A, Faustino MAF, Simões MM, Cavaleiro JA, Nakagaki S, Almeida A, Cunha Â, Silvestre AJD, Freire CS, Pinto RJ, Neves MGPMS. Control of Listeria innocua biofilms by biocompatible photodynamic antifouling chitosan based materials. Dye Pigment 2017;137:265–76. https://doi.org/10.1016/j.dyepig.2016.10.020.
[81] Carvalho CMB, Alves E, Costa L, Tomé JPC, Faustino MAF, Neves MGPMS, Tomé AC, Cavaleiro JAS, Almeida A, Cunha Â, Lin Z, Rocha J. Functional cationic nanomagnet−porphyrin hybrids for the photoinactivation of microorganisms. ACS Nano 2010;4:7133–40. https://doi.org/10.1021/nn1026092.
[82] Ma M, Zhao J, Zeng Z, Wan D, Yu P, Cheng D, Gong D, Deng S. Antibacterial activity and membrane-disrupting mechanism of monocaprin against Escherichia coli and its application in apple and carrot juices. LWT 2020;131:109794. https://doi.org/10.1016/j.lwt.2020.109794.
[83] Rafeeq S, Shiroodi S, Schwarz MH, Nitin N, Ovissipour R. Inactivation of Aeromonas hydrophila and Vibrio parahaemolyticus by curcumin-mediated photosensitization and nanobubble-ultrasonication approaches. Foods 2020;9. https://doi.org/10.3390/foods9091306.
[84] Wang F, Wang R, Pan Y, Du M, Zhao Y, Liu H. Gelatin/Chitosan films incorporated with curcumin based on photodynamic inactivation technology for antibacterial food packaging. Polymers 2022;14. https://doi.org/10.3390/polym14081600.
[85] Kumar A, Ghate V, Kim MJ, Zhou W, Khoo GH, Yuk HG. Antibacterial efficacy of 405, 460 and 520 nm light emitting diodes on Lactobacillus plantarum, Staphylococcus aureus and Vibrio parahaemolyticus. J Appl Microbiol 2016;120:49–56. https://doi.org/10.1111/jam.12975.
[86] Lambert MA, Hickman-Brenner FW, Farmer JJ, Moss CW. Differentiation of Vibrionaceae species by their cellular fatty acid composition. Int J Syst Evol Microbiol 1983;33:777–92. https://doi.org/10.1099/00207713-33-4-777.
[87] Phuoc NN, Richards R, Crumlish M. Establishing bacterial infectivity models in striped Catfish Pangasianodon hypophthalmus (Sauvage) with Edwardsiella ictaluri. J Fish Dis 2020;43:371–8. https://doi.org/10.1111/jfd.13135.
[88] Huang J, Chen B, Zeng Q-H, Liu Y, Liu H, Zhao Y, Wang JJ. Application of the curcumin-mediated photodynamic inactivation for preserving the storage quality of salmon contaminated with L. monocytogenes. Food Chem 2021;359:129974. https://doi.org/10.1016/j.foodchem.2021.129974.
[89] Zhang H, Salo D, Kim DM, Komarov S, Tai Y-C, Berezin MY. Penetration depth of photons in biological tissues from hyperspectral imaging in shortwave infrared in transmission and reflection geometries. J Biomed Opt 2016;21:126006. https://doi.org/10.1117/1.JBO.21.12.126006.
[90] Wong T-W, Wang Y-Y, Sheu H-M, Chuang Y-C. Bactericidal effects of toluidine blue-mediated photodynamic action on *Vibrio vulnificus*. Antimicrob Agents Chemother 2005;49:895–902. https://doi.org/10.1128/aac.49.3.895-902.2005.
[91] Boukani PH, Farahpour MR, Hamishehkar H. A novel multifaceted approach for infected wound healing: optimization and in vivo evaluation of Phenethyl alcohol loaded nanoliposomes hydrogel. J Drug Deliv Sci Technol 2022;77:103888. https://doi.org/10.1016/j.jddst.2022.103888.
[92] Lopes P, Joaquinito ASM, Ribeiro A, Moura NMM, Gomes ATP, Guerreiro SG, Faustino MAF, Almeida A, Ferreira P, Coimbra MA, Neves MGPMS, Gonçalves I. Starch-based films doped with porphyrinoid photosensitizers for active skin wound healing. Carbohydr Polym 2023;313:120894. https://doi.org/10.1016/j.carbpol.2023.120894.
[93] Song Y, Dong X, Hu G. Transcriptome analysis of turbot (Scophthalmus maximus) head kidney and liver reveals immune mechanism in response to Vibrio anguillarum infection. J Fish Dis 2022;45:1045–57. https://doi.org/10.1111/jfd.13628.
[94] Cai X, Gao C, Lymbery AJ, Ma L, Fu Q, Huang R, Li C. LncRNA activates immune response against Vibrio anguillarum in the intestine-liver axis of turbot

(Scophthalmus maximus L.) by sponging miRNA in a ceRNA regulatory network. Aquaculture 2023;576:739882. https://doi.org/10.1016/j.aquaculture.2023.739882.

[95] Song Y, Soomro MA, Dong X, Hu G. Transcriptome analysis reveals immune-related genes in tissues of Vibrio anguillarum-infected turbot Scophthalmus maximus. J Oceanol Limnol 2024;42:332–44. https://doi.org/10.1007/s00343-023-2363-7.

[96] Sanches-Fernandes GMM, Sá-Correia I, Costa R. Vibriosis outbreaks in aquaculture: addressing environmental and public health concerns and preventive therapies using gilthead seabream farming as a model system. Front Microbiol 2022;13:904815. https://doi.org/10.3389/fmicb.2022.904815.

[97] Tannenbaum J, Bennett BT. Russell and Burch's 3Rs then and now: the need for clarity in definition and purpose. J Am Assoc Lab Anim Sci 2015;54:120–32.